Experimental Approach for the Fast Walking by the Biped Walking Robot MARI-1

Youji Nakajima* Akira Yonemura Atsuo Kawamura

Dept. of Elec. and Comp. Eng., Yokohama National University
79-5 Tokiwadai, Hodogaya-ku Yokohama JAPAN
tel:+81-45-339-4162; fax:+81-45-338-1157; e-mail:yonemura@kawalab.ynu.dnj.ac.jp

Abstract: We have developed the biped walking robot "MARI-1". The robot has the light weight and 6 joints on each leg and all control calculation is done with a DSP. The walking pattern is made from the tip position and direction references in X-Y-Z domain and those references are transformed into joint angle references by the inverse kinematics calculation. The position control of each joint is done with the high gain P control.

In this paper, we tried an open-loop type walking. As a result, the quasi-dynamic walking was confirmed by checking the position of the center of the mass(COM). The smooth walking and fast walking are also achieved with the proposed walking pattern.

1 Introduction

It is thought that the humanoid type robot is the best form to work in the human living environment. In the future, it is expected to apply it in various industrial area for a substitute of a part of human work. Thus in many palces, the biped walking robot is studied[1].

Honda has developed the P2 on 1996, and the P3 on 1997[2]. The height of P2 is 1.82[m] and the weight is 210[kg]. The height of P3 is 1.6[m] and the weight is 130[kg]. And Waseda Univercity has developed WABIAN on 1998[3]. The height of WABIAN is 1.66[m] and the weight is 107[kg]. Both robot is made of aluminum or magnesium. The weight of the robot is very heavy.

MARI-1 has been developed in our laboratory[4][10]. MARI-1 is made of mono cast nylon. Thus the weight is very light, which is 25[kg] and the hight is 1.21[m]. The weight is very light compared with the height, thus the less power is needed to make the robot walk and this robot seems safe even if it is in the human living environment.

2 Hardware Design and Control System

2.1 Frame Design

The robot has 6 joints on each leg, and each feet can take any position and posture in the 3-dimentional space.

The frame of the robot is made of the mono cast nylon. The density of mono cast nylon is little heavy compare with water. And it has tough mechanical strength and endurance . MARI-1 is very light weight due to this material. The height of the robot is 1.21[m], the weight is 25[kg]. The appearance of the robot is shown in Fig.1. The controllers are located outside of the robot, thus many wires are connected.

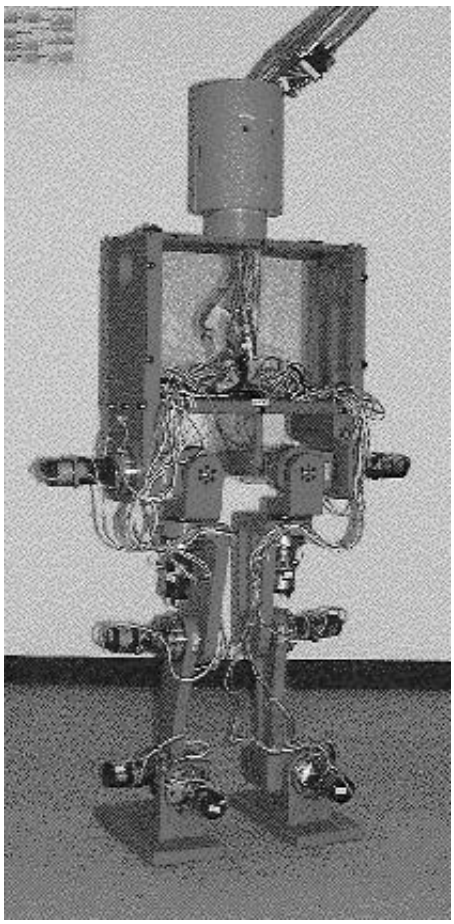

Fig.1: Biped Walking Robot MARI-1

And the demension of the robot is shown in Fig.2. The thickness of the frame is 20[mm]. The foot size is 250[mm] $\times$ 120[mm] for a stable walking.

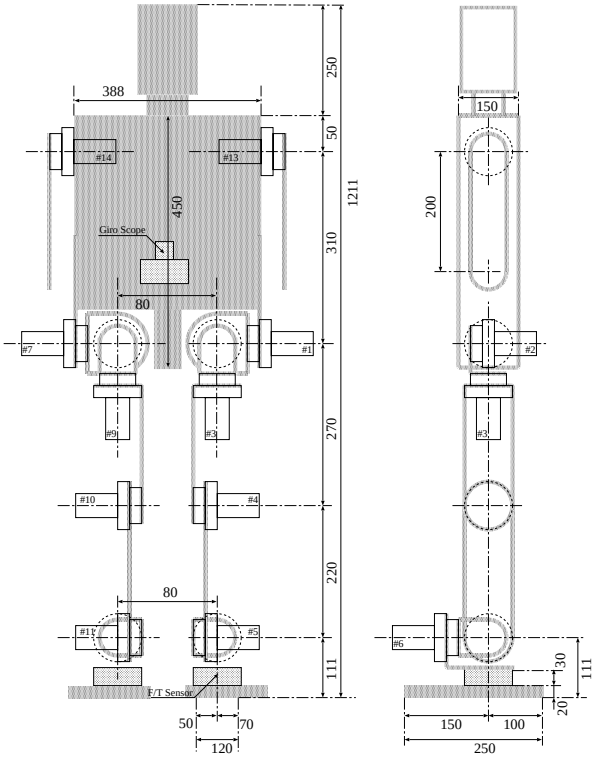

Fig.2: Dimension of the Robot

2.2 Motors And Gears

At the initial design DC servo motors with 50:1 harmonic gears were used as the actuators, which have rotary encoders. The rated power and torque of the motors were estimated by the simulator(ROCOS) and the results in Table2 was obtained[4] [5]. Joint numbers are shown in Fig.3. The dotted lines denote the directions of the rotation axes of the joint motors.

Here the rated value means the average value. Then DC motors were selected as shown in Table1.

Table 1: Selected motors

Joint No.	1	2, 4	3, 5	6
Rated Power[W]	60	40	23	11
Rated Torque[N · m]	9.3	6.6	3.7	1.76
Peak Torque [N · m]	62.2	39.2	21.1	7.4

The robot was made with these motors. However in the experiments, it was found the motor power and the torque was not large enough. Thus ankle motors were chaneged for bigger power ones. Exchaneged motors are shown in Table3. Also all harmonic gears were exchanged to 100:1.

Table 2: Estimated rated power and torque

Joint No.	1	2	3	4	5	6
Rated Power[W]	80	17	12	37	28	4
Rated Torque[N · m]	42	41	24	45	22	11

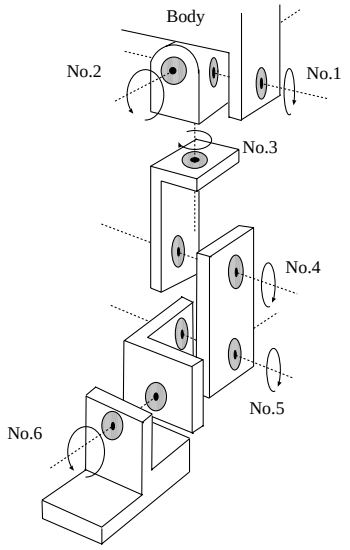

Fig.3: Joints of the foot

Table 3: New selection of motors

Joint No.	1	2	3	4	5	6
Power(before)[W]	60	40	23	40	23	11
Power(after)[W]	60	40	23	40	40	23

2.3 Control System

All calculation of the control is done by one DSP board with the TMS320C32-50MHz. The walking programs are developed on the host computer by the C language. The control system is shown in Fig.4. In this experiments, we only use the function of the dotted line section.

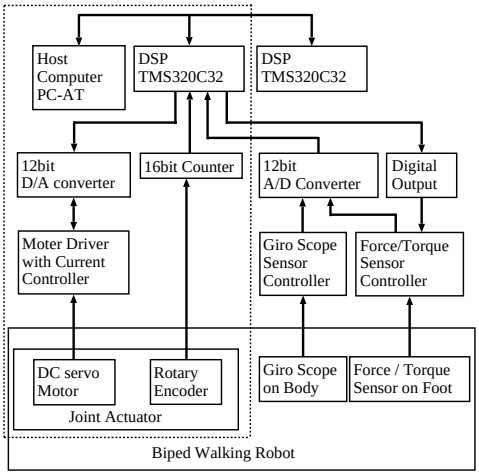

Fig.4: Control system

3 Walking Pattern

3.1 Inverse Kinematics

When we make the robot walk, we must think the tip position and direction references of the both feet in the X-Y-Z domain.

Joint angle references can be obtained to transform the tip position and direction references by the inverse

kinematics calculation. In this experiments, the inverse kinematics calculation is made by the Newton-Raphson method. The coordinates about the kinematics of the robot is shown in Fig.5. This figure shows only a right foot case.

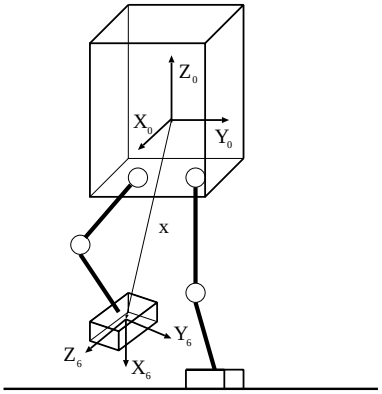

Fig.5: Kinematics of the robot

There are 6 coordinates on each foot. Each coordinate is placed on each joint. The base coordinate is the body-fixed one X_0 - Y_0 - Z_0. The relationship from the body-fixed coordinate to the tip fixed coordinate X_6 - Y_6 - Z_6 can be described by the calcuration of the coordinates transformation. Tip position refernces are given by the tip position vector $\mathbf{x} = \{x, y, z\}$, and direction references by the posture matrix $\mathbf{A}$

$$\mathbf{A} = \begin{bmatrix} a_{11} & a_{12} & a_{13} \\ a_{21} & a_{22} & a_{23} \\ a_{31} & a_{32} & a_{33} \end{bmatrix} \tag{1}$$

The first row vector $\mathbf{a}_x = \{a_{11}, a_{21}, a_{31}\}^T$ is the unit vector which denotes where the X_6 axis points with respect to the body-fixed coodinate. Similarly, the second row vector $\mathbf{a}_y$ and the third row vector $\mathbf{a}_z$ denotes the direction of Y_6 and Z_6 axes.

Tip position and direction references are transformed into joint angle references by the inverse kinematics calculation as follows.

Suppose the reference $\mathbf{q}_{ref} = \{\mathbf{x}_{ref}, \mathbf{A}_{ref}\}$. Then the position and the direction error vectors become

$$\mathbf{e}_x = \mathbf{x}_{ref} - \mathbf{x} \tag{2}$$

$$\mathbf{e}_d = \frac{1}{2}(\mathbf{a}_x \times \mathbf{a}_{xref} + \mathbf{a}_y \times \mathbf{a}_{yref} + \mathbf{a}_z \times \mathbf{a}_{zref}) \tag{3}$$

Joint angle reference $\theta = \{\theta_1, \theta_2, \theta_3, \theta_4, \theta_5, \theta_6\}$ can be obtained by the Newton-Raphson method.

$$\theta_{n-1} = \theta_n + \mathbf{J}_n^{-1}\mathbf{e}_n \quad (n = 1, 2, \cdots) \tag{4}$$

where

$$\mathbf{e} = \begin{pmatrix} \mathbf{e}_x \\ \mathbf{e}_d \end{pmatrix} \tag{5}$$

and $\mathbf{J}(\theta)$ denotes the Jacobian matrix

$$\mathbf{J}(\theta) = -\frac{\partial \mathbf{e}}{\partial \theta^T} \tag{6}$$

3.2 Generation of the Walking Pattern

When the walking pattern is generated, position references $\mathbf{x}_{ref} = \{x, y, z\}$ in the X-Y-Z domain are decided first. Position references are given with respect to the body-fixed coordinate shown in Fig.5.

The orbits of the tip in X, Y and Z direction are given as the function of the time. The orbit in the X direction is shown in Fig.6. The footstep slide s in the X direction is decided first and the orbit beteween each point is connected through the sine curve.

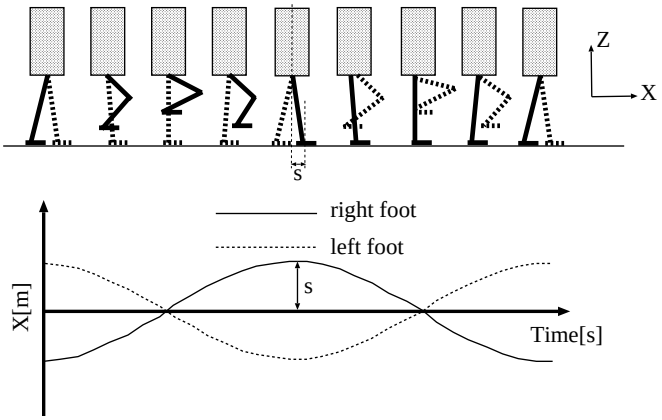

Fig.6: Orbit of X direction

The orbit in Y direction is shown in Fig.7. The distance d of the motion in the Y direction is decided first and the orbit is generated similarly.

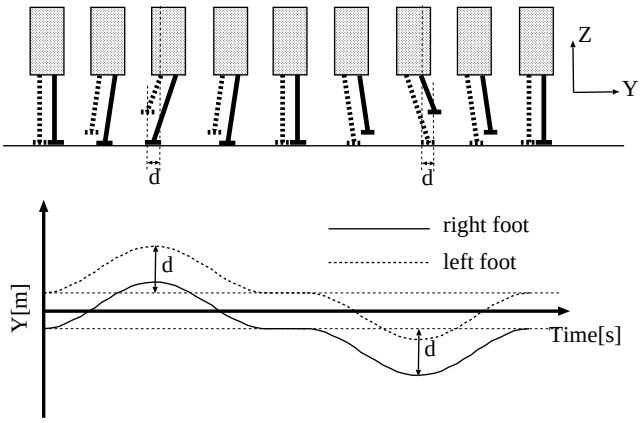

Fig.7: Orbit of Y direction

The orbit in the Z direction is shown in Fig.8. The height h to which the robot raises its foot is decided first and the orbit is generated similarly.

In this experiments, the feet of the robot were kept horizontal against the ground. Thus direction references $\mathbf{A}$ was given as follows:

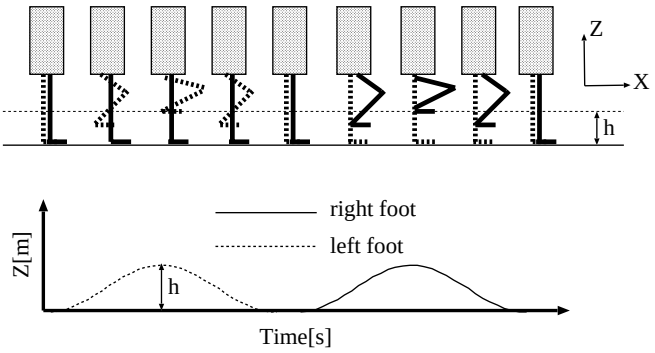

Fig.8: Orbit of Z direction

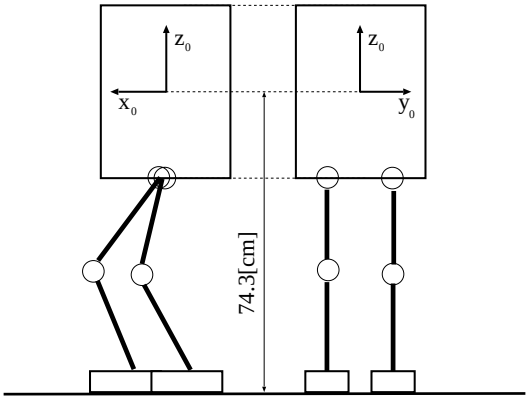

Fig.9: Initial posture

$$\mathbf{A} = \begin{bmatrix} 0 & 0 & 1 \\ 0 & 1 & 0 \\ -1 & 0 & 0 \end{bmatrix} \tag{7}$$

The experiments was made with various values of the parameters of the walking pattern. The values of the parameters were decided through the experiments by trial and error.

3.3 Servo Control of Each Joint

Before the remake of the robot, the PID control, the disturbance observer and the H_∞ control were used as the joint position control. But when the motors were overloaded, joint angle errors were integrated and the tracking response to the position reference was not satisfactory. Thus the high gain P control is used. In this experiments, the same high gain P control is also used.

3.4 How to give the references

Tip position and direction references are made and transformed into joint angle references in abovementioned method. Those references are generated at every 0.01[s]. All joint angle refernces are sent to the walking program which is downloaded to the DSP. These calculations are done off-line.

Before the walking, the robot has the initial posture first. The initial posture is shown in Fig.9. And the robot starts walking with given joint angle refernces.

4 Experimental Results

In the present walking experiment system, the following data can be measured.

1. joint angles
2. motor current references on each joint
3. position of COM(the centor of the mass)

The following discussion is done with these data.

4.1 Quasi-Dynamic Walking

It is well known that there are two kind of biped walking. One is the static walking and the other is the quasi-dynamic walking. The quasi-dynamic walking has the faster walking speed and requires the less energy. If we can make the robot walk in the quasi-dynamic walking, it can be said that the better walking is realized.

We inspect if our biped walking satisfies the condition of the quasi-dynamic walking. In the case of the static walking, COM is always in the range of the foot width of the support leg. If the robot can walk stably when the position of COM is not in the range of the foot, it can be said that the robot makes the quasi-dynamic walking.

Parameters of the walking pattern used in the experiment are shown in Table4. The range of the foot of support leg and the position of COM in the x direction is shown in Fig.10.

Table 4: Parameters of the experiment

Footstep slide s [cm] in x direction	7.0
Distance d [cm] in y direction	7.8
Height h [cm]in z direction	3.2
Period [s]	0.8

The solid line denotes the position of COM. One dotted line denotes the inside edge of the foot of the support leg, and another denotes the outside edge. The painted area denotes the support polygon.

In Fig.10, the position of COM is not always in the support polygon. Before and after of the change the support leg to the other free leg, the period that the position of COM is out from the support polygon exists. The robot walked stably in all the moment of this walking pattern. Thus it is confirmed that the robot did the quasi-dynamic walking.

4.2 Calculated ZMP from the axis position

The position of COM in section 4.1 is not always located in the support polygon. In this section, the ZMP is calculated from the mesured axis positions.

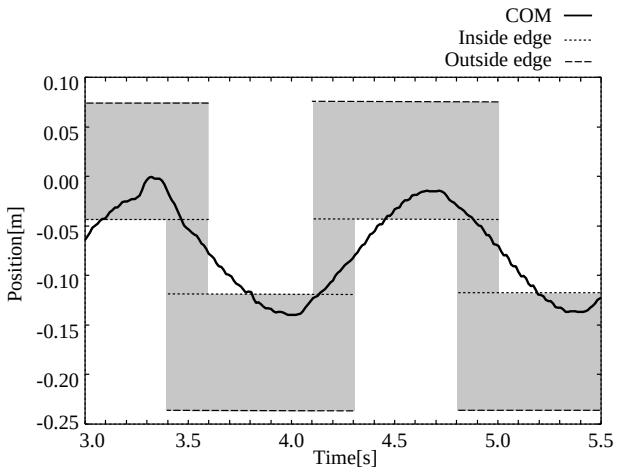

Fig.10: Range of the foot and the position of COM

The two dimensinal ZMP is given in [11].

$$X_{ZMP} = \frac{\sum_{k=0}^{n} m_k(z_k'' + g_z)x_k - \sum_{k=0}^{n} m_k(x_k'' + g_x)z_k}{\sum_{k=0}^{n} m_k(z_k'' + g_z)} \quad (8)$$

$$Y_{ZMP} = \frac{\sum_{k=0}^{n} m_k(z_k'' + g_z)y_k - \sum_{k=0}^{n} m_k(x_k'' + g_y)z_k}{\sum_{k=0}^{n} m_k(z_k'' + g_z)} \quad (9)$$

Where m_k is the mass of kth link, x_k, y_k, z_k is the (x, y, z) position mesured from the support leg tip. $''$ is the second derivative, and g_z is the gravity.
When the coordinate is shifted to the center of the body (COB),(8)(9) are modified to the following.

$$\overline{X}_{ZMP} = \frac{[\sum_{k=0}^{n} m_k(\overline{z}_k'' + z_q'' + g_z)\overline{x}_k - \sum_{k=0}^{n} m_k(\overline{x}_k'' + x_q'' + g_x)(\overline{z}_k + z_q)]}{\sum_{k=0}^{n} m_k(\overline{z}_k'' + z_q'' + g_z)} \quad (10)$$

$$\overline{Y}_{ZMP} = \frac{[\sum_{k=0}^{n} m_k(\overline{z}_k'' + z_q'' + g_z)\overline{y}_k - \sum_{k=0}^{n} m_k(\overline{y}_k'' + y_q'' + g_y)(\overline{z}_k + z_q)]}{\sum_{k=0}^{n} m_k(\overline{z}_k'' + z_q'' + g_z)} \quad (11)$$

Where (x_q, y_q, z_q) is the position of COB mesured from the support leg tip.$(\overline{x}_k, \overline{y}_k, \overline{z}_k)$ is the position of the kth link mesured from the COB. Parameters for the walking patterns are the same as Table 4.
The range of thefoot of support leg, the position of COM and the position of ZMP in x direction are shown in Fig11. The solid line denotes the position of ZMP.One doted line denotes the position of COM. Two doted line denotes the inside edge of the foot of the support leg, and another denotes the outside edge. The shadowed area denotes the support polygon. In Fig11, the position of ZMP is not always in the support polygon. When the robot lifts the free leg, or just when the free leg touches down the floor, the ZMP approaches to the inside edge of the support leg. And for a short period, the ZMP moves to outside of the sole in Fig11.This is because the sole size is assumed to be large enough in (10) and (11). The practical understanding is that for this short period, the robot leans to the free leg direction, and the outside edge of the support leg sole does not fit to the floor. Authors are now investigating the better wallking pattern from the view point of ZMP.

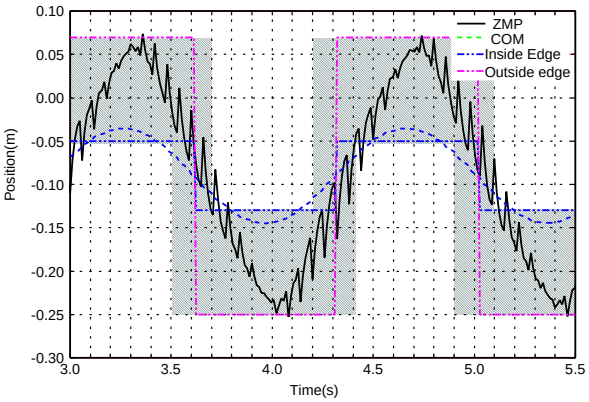

Fig.11: Range of the Foot and the position of ZMP

4.3 Effectiveness of the Servo Control

The waveforms of a joint angle θ and a joint angle reference θ_{ref} are shown in Fig.12. The high gain P control works without the error divergence and joint angle errors were kept small.

4.4 Pattern For Better Walking

We made the experiments with various values of the parameters. When parameters are changed, the state of the walking changed. In this section, we make the two kind of estimation.

4.4.1 Smooth Walking

If the required power for joints becomes large, the walking becomes unstable and the robot falls to the ground. To avoid the phenomena, we selected the walking pattern so that the less power is consumed. We select

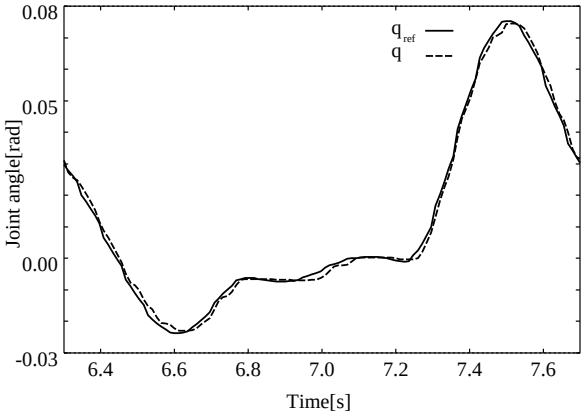

Fig.12: Joint angle references and joint angles at θ_4

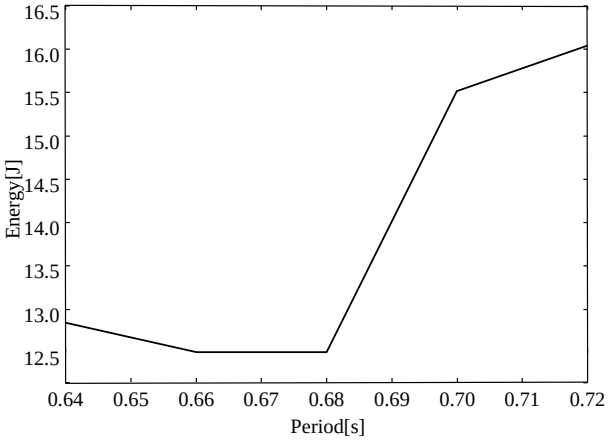

Fig.14: Approximated power of joint No.2

the maximum current refernce of the motor as the one performance index for the less power walking.

The footstep slide $s = 5.0[cm]$, the distance $d = 7.6[cm]$ and the height $h = 3.8[cm]$ are kept equal and the period is only changed. The change of the period and the maximum current reference of the joint No.2 of the right leg is shown in Fig.13. And the approximated power of one period of one step is shown in Fig.14.

Around 0.68[s] of one step period, both the maximum current and the power become the least. The robot has its own mechanical resonance frequency. It is thought that the frequency 1/0.68[Hz] may be close to the mechanical resonance frequency. If the frequency of the walking pattern is near the mechanical resonance frequency, the robot could walk with the less power.

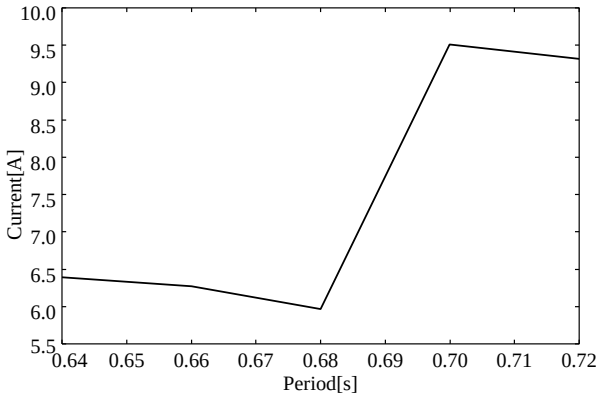

Fig.13: Maximum current of joint No.2

4.4.2 Fast Walking

As another performance index, the speed of the walking is selected. The height $h = 3.8[cm]$ and the period $T = 0.7[s]$ are kept equal and the footstep slide s is changed. The distance d is changed according to the change of the footstep slide s. The change of the footstep slide and the maximum current reference of the joint No.2 of the right leg is shown in Fig.15. And the approximated power of one period is shown in Fig.16. And the maximum current refernce and approximated power of the joint No.4 are shown in Fig.17, and Fig.18.

The rotation axis of the joint No.2 is the roll axis. Thus it is thought that the variation of the current does not have so many relationship with the variation of the footstep slide. On the other hand, the rotation axis of the joint No.4 is the pitch axis. Thus the current increses as the footstep slide become large. Since the current limit of the motor on the joint No.4 is 16[A], the maximum current refernce must be kept less than 16[A].

5 Conclusion

We developed the biped walking robot MARI-1 and remade the frame of the robot and the motors with harmonic gears. And we made the biped walking experiments. We suceeded in making the robot do the quasi-dynamic walking. And also we investigated the smooth walking and the fast walking.

In future, we plan to make the robot walk faster and we will consider the walking pattern which has the minimum power for joint motors.

And we plan to put the sensors on the robot and do the feedback control from the information of the acceleration, gyro, and force sensors.

References

[1] Special Issue: Walking Robot, *Jarnal of the Robotics Society Japan*, Vol.11, No.3, pp.305-394, 1993.

[2] M. HIROSE, T. TAKENAKA, H. GOMI and N. OZAWA, "Humanoid Robot", *Jarnal of the Robotics Society Japan*, Vol.15, No.7, pp.983-985, 1997.

[3] J. YAMAGUCHI, S. INOUE, D. NISINO, S. GEN, A. ISHII, S. MATSUO, Y. YAMAMOTO, H. OZAWA, A. TAKANISHI, "Development of the Waseda Biped Humanoid Robot WABIAN -Design method of the total system- ", *Proceedings of the 15th Annual Conference of*

the Robotics Society of Japan, vol.3, pp.773-774, September 1997.

[4] Y. FUJIMOTO, "Study on Biped Walking Robot with Environmental Force Interaction" *Doctoral Thesis*, pp.5-24, 49-52, March 1998.

[5] Y. FUJIMOTO, A. KAWAMURA, "Autonomous Control of 3D Dynamics Simulations of Biped Walking Robot", *IEEE Robotics and Automation Magazine*, Vol.5, No.2, pp.33-42, 1998.

[6] Robotics Society Japan, "Robotics Handbook", CORONA PUBLISHING CO., LTD., pp.181-402, 1990.

[7] J.J. Craig, "Introduction to Robotics", Addison-Wesley Publishing Company, 1989.

[8] S. KAJITA, A. KOBAYASHI, "Dynamic Walk Control of a Biped Robot with Potential Energy Conserving Orbit", *SICE*, Vol.23, No.3, pp281-287, March 1987.

[9] Y. FUJIMOTO, A. KAWAMURA, "Robust Biped Walking Active Interaction Control between Foot and Ground", *ICRA*, pp.2030-2033, 1998.

[10] A.YONEMURA, Y.NAKAJIMA, A.HIRAKAWA, A. KAWAMURA, "Experimental Approach for the Biped Walking Robot MARI-1", *AMC*, pp.548-553, 2000.

[11] A.TAKANISHI,"Biped Walking Robot Compensating Moment by Trunk Motion", *Journal of RSJ*, pp.348-353, Vol.11, No.3, pp.348-353, 1993.

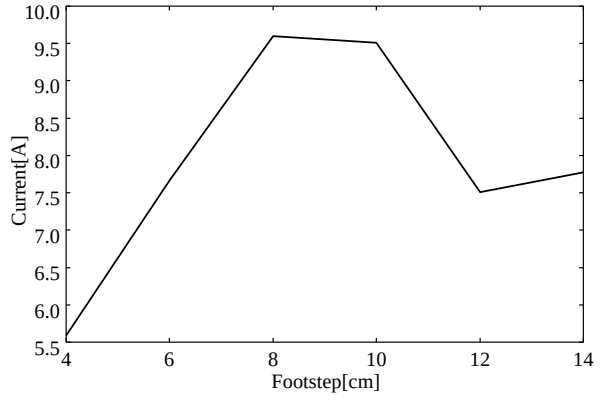

Fig.15: Maximum current of joint No.2

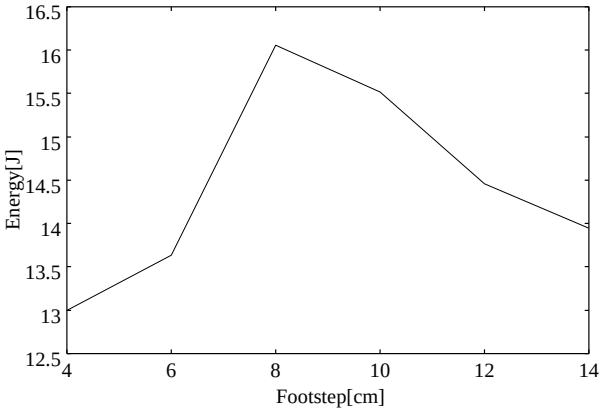

Fig.16: Approximated power of joint No.2

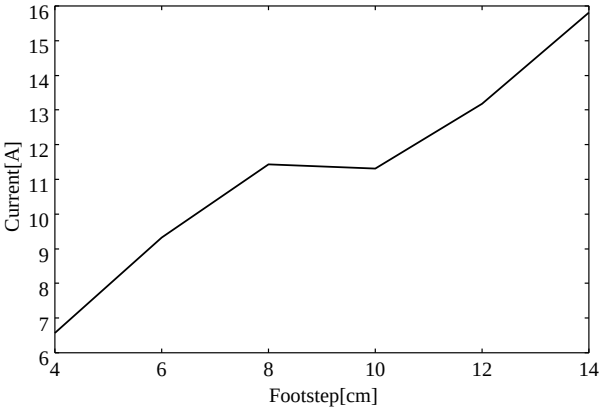

Fig.17: Maximum current of joint No.4

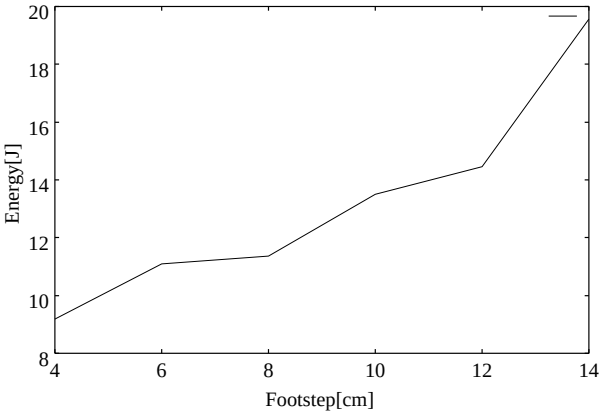

Fig.18: Approximated power of joint No.4